

<https://doi.org/10.1038/s41541-024-01051-3>

Identifying falsified COVID-19 vaccines by analysing vaccine vial label and excipient profiles using MALDI-ToF mass spectrometry



A list of authors and their affiliations appears at the end of the paper

The rapid development and worldwide distribution of COVID-19 vaccines is a remarkable achievement of biomedical research and logistical implementation. However, these developments are associated with the risk of a surge of substandard and falsified (SF) vaccines, as illustrated by the 184 incidents with SF and diverted COVID-19 vaccines which have been reported during the pandemic in 48 countries, with a paucity of methods for their detection in supply chains. In this context, matrix-assisted laser desorption ionisation-time of flight (MALDI-ToF) mass spectrometry (MS) is globally available for fast and accurate analysis of bacteria in patient samples, offering a potentially accessible solution to identify SF vaccines. We analysed the COVISHIELD™ COVID-19 vaccine; falsified versions of which were found in India, Myanmar and Uganda. We demonstrate for the first time that analysis of spectra from the vaccine vial label and its adhesive could be used as a novel approach to detect falsified vaccines. Vials tested by this approach could be retained in the supply chain since it is non-invasive. We also assessed whether MALDI-ToF MS could be used to distinguish the COVISHIELD™ vaccine from surrogates of falsified vaccines and the effect of temperature on vaccine stability. Both polysorbate 80 and L-histidine excipients of the genuine vaccine could be detected by the presence of a unique combination of MALDI-ToF MS peaks which allowed us to distinguish between the genuine vaccines and falsified vaccine surrogates. Furthermore, even if a falsified product contained polysorbate 80 at the same concentration as used in the genuine vaccine, the characteristic spectral profile of polysorbate 80 used in genuine products is a reliable internal marker for vaccine authenticity. Our findings demonstrate that MALDI-ToF MS analysis of extracts from vial labels and the vaccine excipients themselves can be used independently to detect falsified vaccines. This approach has the potential to be integrated into the national regulatory standards and WHO's Prevent, Detect, and Respond strategy as a novel effective tool for detecting falsified vaccines.

The rapid development of vaccines against coronavirus disease 2019 (COVID-19) was a remarkable success in biomedical research marked by the supply and distribution worldwide, with billions of doses administered¹. However, the vital importance but inequitable global distribution of COVID-19 vaccines has been associated with increasing concerns about the occurrence and impact of substandard and falsified (SF) vaccines^{2–4}. According to the World Health Organization (WHO), approximately 10% of medical products distributed in low- and middle-income countries

(LMIC) are either substandard or falsified^{5,6}. This concerning estimate suggests a significant but neglected risk, potentially leading to higher rates of illness and death, as well as eroding public trust in healthcare systems and economic harm. In light of the growing recognition of the importance of vaccines in the fight against diseases, this issue becomes even more significant.

Substandard or 'out of specification' products are authorised medical products that fail to meet either their quality standards or specifications, or

✉ e-mail: paul.newton@ndm.ox.ac.uk; bevin.gangadharan@bioch.ox.ac.uk

both. If the vaccine cold chain is not maintained in the supply chain (e.g. if left at ambient temperature which can be above 45 °C in some countries) this is likely to result in a poor-quality substandard vaccine. In contrast, falsified products refer to products that deliberately or fraudulently misrepresent their identity, composition or source⁶.

SF medical products pose a significant threat to health as they are of poor quality, unsafe and/or ineffective⁷. Moreover, there is inadequate recognition of the scale of the problem or of the need to establish appropriate risk analysis, monitoring and intervention systems. In the public domain, there have been reports of 184 incidents of diverted and SF COVID-19 vaccines from 48 countries and most cases of vaccine falsification have been in LMIC⁸. In one of these 184 incidents alone, 2,500 people were wrongly injected with saline as a fake instead of the genuine COVID-19 vaccine⁹. In other cases, 6,000 vials of falsified COVISHIELD™ COVID-19 vaccine (equivalent to 60,000 doses) were seized in Varanasi¹⁰ and a member of the Indian parliament (along with a few hundred other individuals) was injected with falsified COVISHIELD™¹¹. Other COVID-19 vaccines have also been falsified including the Oxford AstraZeneca vaccine (in Iran)¹² and Pfizer-BioNTech Comirnaty® vaccine (in Poland, Mexico and Iran)^{13,14}. Before the pandemic, multiple non-COVID-19 vaccines had also been falsified including vaccines for cholera (Dukoral® in Bangladesh), rabies (Verorab® in Philippines) and meningitis (Mencevax® in Niger)¹⁵.

There are no readily available devices currently being used in the supply chain to screen for SF vaccines. Such devices are required to empower inspectors and enforcement agencies conducting risk-based post-market surveillance, that could be integrated into the national regulatory standards and WHO's Prevent, Detect, and Respond strategy². The risk of SF vaccines in the pandemic spawned increased interest, with the evaluation of near-infrared¹⁶, spatially-offset Raman spectroscopy (SORS)¹⁷ and lateral flow test devices¹⁸.

The Vaccine Identity Evaluation Collaboration (<https://www.cgfr.ox.ac.uk/research/medicine-quality-research-group/mqrg-projects/vaccine-identity-evaluation>) has been evaluating a diverse range of screening devices^{17,18} and here we describe the application of matrix-assisted laser desorption ionisation–time-of-flight mass spectrometry (MALDI-ToF MS) which provides spectral information where peaks correspond to the molecular weights of ionised molecules (e.g. proteins and other compounds). MALDI-ToF MS is widely available throughout the world including in some LMIC where they are used in clinical microbiology laboratories for the identification and speciation of micro-organisms¹⁹ and other specific purposes, such as to identify proteins in influenza virus vaccines²⁰. We have recently established a MALDI-ToF MS method to differentiate genuine non-Covid vaccines from falsified vaccine surrogates²¹. However, there has been no published literature reporting the use of MALDI-ToF MS to analyse vaccine vial labels, the spectral peak distribution of polysorbate in vaccines or the other constituents of COVID vaccines to help with their authentication.

In this study, we report the application of MALDI-ToF MS to distinguish genuine COVISHIELD™ (a COVID-19 vaccine manufactured by

Serum Institute India Pvt. Ltd.) from a range of falsified vaccine surrogates. COVISHIELD™ is a recombinant non-replicating chimpanzee adenovirus viral vector (ChAdOx1) vaccine encoding the severe acute respiratory syndrome coronavirus 2 (SARS-CoV-2) Spike glycoprotein²². Falsified COVISHIELD™ vaccine has been identified in Africa (Uganda) and South-East Asia (India and Myanmar)²³. In these cases, the criminals changed the labels in the following ways: falsifying the expiry date (Uganda), stating an incorrect volume of 2 mL with 4 doses instead of 5 mL with 10 doses (India), and falsifying the batch number with an incorrect spelling of vaccine brand as COVISHELD (Myanmar). It is not in the public domain what the criminals used for the falsified labels in the three countries. However, from the photos in the WHO Medical Product Alert²³, it appears as though the labels could have been self-adhesive office labels with the label information printed with an office colour printer.

Since WHO have reported changes in the label for falsified COVISHIELD™ vials which have been seized, we evaluated the use of MALDI-ToF MS to analyse extracts from the COVISHIELD™ labels to see if we could acquire unique spectral fingerprint for the genuine label and its adhesive. The analysis of labels helps to differentiate batches but most importantly is non-invasive and therefore allows the tested vaccine vials, found to be authentic, to be retained in the supply chain. MALDI-ToF MS was also used to analyse the vaccine liquid using our recently reported method²¹ and we have for the first time applied MALDI-ToF MS for a COVID-19 vaccine and evaluated if the method can detect heat exposure degradation (i.e. substandard) vaccines. Furthermore, we show that the distribution of polysorbate 80 spectral peaks acts as an internal marker for vaccine authenticity due to their characteristic peak profiles and significant spectral variations between polysorbate 80 manufacturing sources. Two different MALDI-ToF MS systems were used in this study to compare results - a bioMérieux VITEK® MS and a Bruker Biotyper® Sirius. Both devices are commonly used in hospital microbiology laboratories worldwide making them potentially readily available for vaccine screening programs.

Results

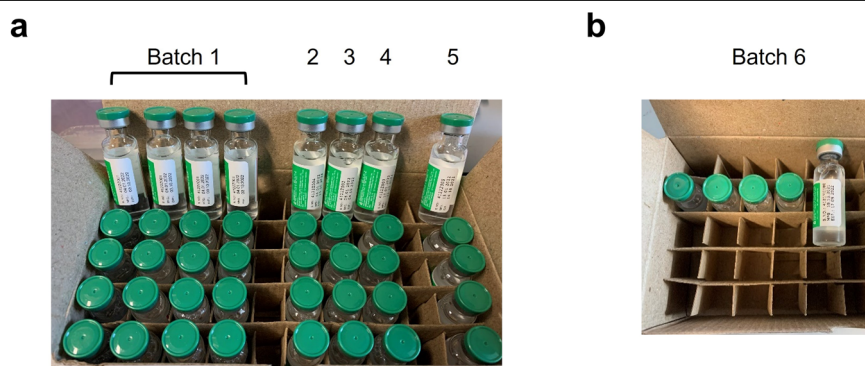
Inter- and intra-batch analyses of COVID-19 vaccine

The inter- and intra-batch analyses were performed on genuine COVISHIELD™ vaccine vials (Fig. 1 and Table 1). Using the peak list generated by Biotyper, principal component analysis (PCA) score plots of the first two most significant principal components showed no differences between batches (Fig. 2a) and between vials with the same batch number (Fig. 2b). These can be observed by the overlapping 95% confidence regions, shown as coloured elliptical areas. Similar results were generated from the analysis of spectra from the Vitek-MS (Supplementary Fig. 1).

Detection of vaccine excipient masses using MALDI-ToF MS

In our attempt to identify COVISHIELD™ vaccine constituents using MALDI-ToF MS, visual inspection of the spectra at 0–900 *m/z* revealed the presence of a peak at 156 *m/z* which corresponded to the nominal mass for the excipient L-histidine (Fig. 3a) that was not detected in the matrix spectra.

Fig. 1 | The genuine Serum Institute India (SII) COVISHIELD™ COVID-19 vaccine samples used in the study. Batches of vaccine samples from (a) Hadapsar factory and (b) Manjari factory were analysed.



L-histidine was made up in water as a standard and analysed by MALDI-ToF MS. As expected, a peak at 156 *m/z* was observed which aligned with the 156 *m/z* for the COVISHIELD™ vaccine. The spectra for the excipient polysorbate 80, which was made up in water as a standard, showed a unique peak at 309 *m/z* (Fig. 3b) and as a series of evenly spaced peaks in the mid-mass range 700–2500 *m/z* (Fig. 4a and Supplementary Fig. 2a) and in the high mass range 2000–20,000 *m/z* (Supplementary Fig. 2b) that were not observed in the matrix spectra but were seen in the genuine COVISHIELD™ vaccine. In the high mass range, most of these evenly spaced peaks for polysorbate 80 in COVISHIELD™ were seen from 2000 to 4,000 *m/z* (Supplementary Fig. 3).

Differentiation of genuine COVISHIELD™ COVID-19 vaccine and surrogates of falsified vaccines

MALDI-ToF MS was used to differentiate between genuine COVISHIELD™ vaccine and surrogates of falsified vaccines (Table 2). Different spectral peaks could be visually observed in the low 0–900 (Fig. 5a) and 700–2500 *m/z* (Fig. 5b) mass ranges when comparing the spectra of the genuine vaccine alongside eight surrogates. Although some peaks overlapped in the spectra between the genuine COVISHIELD™ vaccine and the surrogates at 0–900 *m/z*, there were also peaks unique to COVISHIELD™, such as the peaks mentioned earlier at 156 and 309 *m/z*, specific for L-histidine and polysorbate 80, respectively (Fig. 3a and b). COVISHIELD™ could be readily distinguished from the other surrogates at the mid-mass range (700–2500 *m/z*) (Fig. 5b) and also at the 2000–20,000 *m/z* range that is routinely used in microbial identification (Supplementary Fig. 3). The spectral profile of polysorbate 80 was reproducible among the six batches of COVISHIELD™ vaccine (Supplementary Fig. 4). However, the peaks for poly-

sorbate 80 from other manufacturers were different and could be well separated by PCA (Fig. 4b). The PCA score plots of the first two principal components showed a distinct separation of the COVISHIELD™ vaccine from all falsified vaccine surrogates (Fig. 6a), without any overlap in the 95% confidence regions. This was supported by partial least squares discriminant analysis (PLS-DA) with cross-validation and permutation testing (Fig. 6c–e) which demonstrated perfect separation of all groups (Supplementary Table 1). To confirm the robustness of the PLS-DA model and investigate its potential to identify vaccine surrogates from previously unseen data, an external validation was applied by splitting the data into training (80%) and test (20%) sets. This model was able to distinguish between COVISHIELD™ vaccine from all falsified vaccine surrogates with 100% accuracy in both the training and the external validation test sets with a 90/10 split (Supplementary Table 1). In addition to this 90/10 split, a 70/30 split was also carried out also showing perfect accuracy for the genuine vaccine (data not shown).

Amikacin has been reported to be used as falsified COVISHIELD™ COVID-19 vaccines intercepted in India during the pandemic⁸. When analyzing only COVISHIELD™ and amikacin, the PCA scores plots could differentiate between them (Fig. 6b and Supplementary Fig. 5b). This was also supported by the PLS-DA scores plot with good cross-validation (high accuracy, R², and Q² scores) and significant permutation test (*p* < 0.05) results (Fig. 6c–e) and perfect accuracy of external validation confusion matrices (Supplementary Table 1). Dendrogram analysis revealed the clustering of COVISHIELD™ samples into a monophyletic group (Fig. 7 and Supplementary Fig. 6). Other surrogates also clustered into separate groups in the dendrogram, except for the Milli-Q water and water for injection since both are purified water and, as expected, had similar spectra (Fig. 6a, Fig. 6c, Fig. 7 and Supplementary Fig. 5a).

Table 1 | COVISHIELD™ vaccine samples batch numbers from Hadapsar factory (Batch 1–5) and Manjari factory (Batch 6) in India, used in the study

| Batch group | Vaccine batch number | Number of vials |
|-------------|----------------------|-----------------|
| Batch 1 | 4122Z001 | 20 |
| Batch 2 | 4122Z002 | 5 |
| Batch 3 | 4122Z003 | 5 |
| Batch 4 | 4122Z004 | 5 |
| Batch 5 | 4122Z005 | 5 |
| Batch 6 | 4121MC180 | 5 |

Effect of temperature degradation on genuine COVID-19 vaccine

In order to explore vaccine degradation, vaccine samples were exposed to different temperature conditions followed by comparison using MALDI-ToF analysis. Multivariate analysis of vaccine spectra showed no difference between degradation conditions, as depicted as the plotting of samples with overlapping 95% confidence region of PCA (Fig. 8a). Further, PLS-DA resulted in a non-significant model (Fig. 8b) with low cross-validation scores (Fig. 8c) and non-significant permutation test (Fig. 8d). The high R² of this model and accuracy of the model on training data (Supplementary Table 2) is consistent with overfitting as confirmed by external validation which resulting in an accuracy of only 75% on the test set (Supplementary Table 2). No significant differences were observed when analysing spectra from

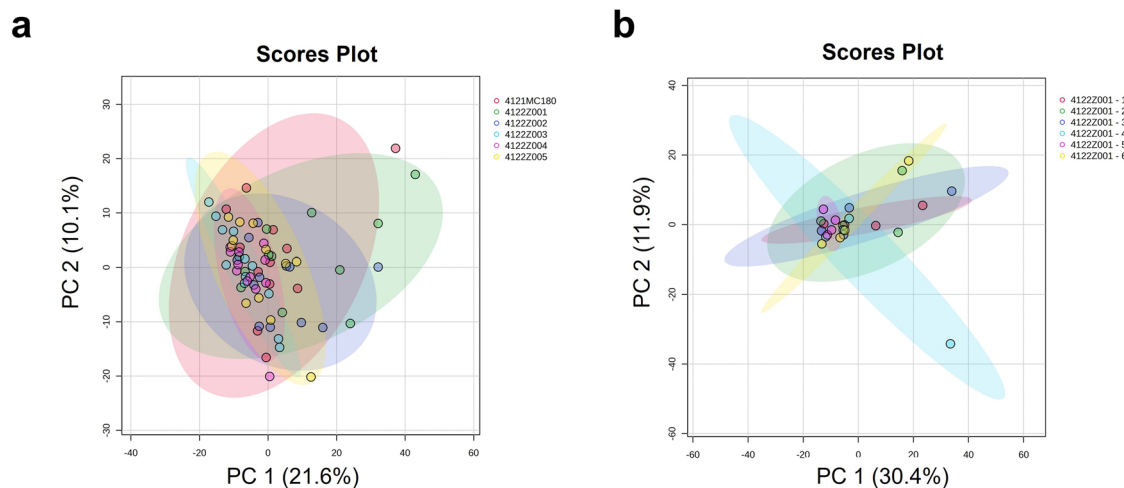


Fig. 2 | Multivariate analyses of the MALDI-ToF MS spectra generated from COVISHIELD™ COVID-19 vaccine samples. PCA score plots were generated for a Six different batch numbers of COVISHIELD™ vaccine (inter-batch analysis, *n* = 3) for each batch number, with four technical replicates for each *n*, generating a total of

12 spectra replicates; and **b** Six vaccine vials of the same batch number 4122Z001 (intra-batch analysis, *n* = 3). Each vial had 4 technical replicates. Spectra generated using Biotyper MALDI-ToF MS at 0–900 *m/z*.

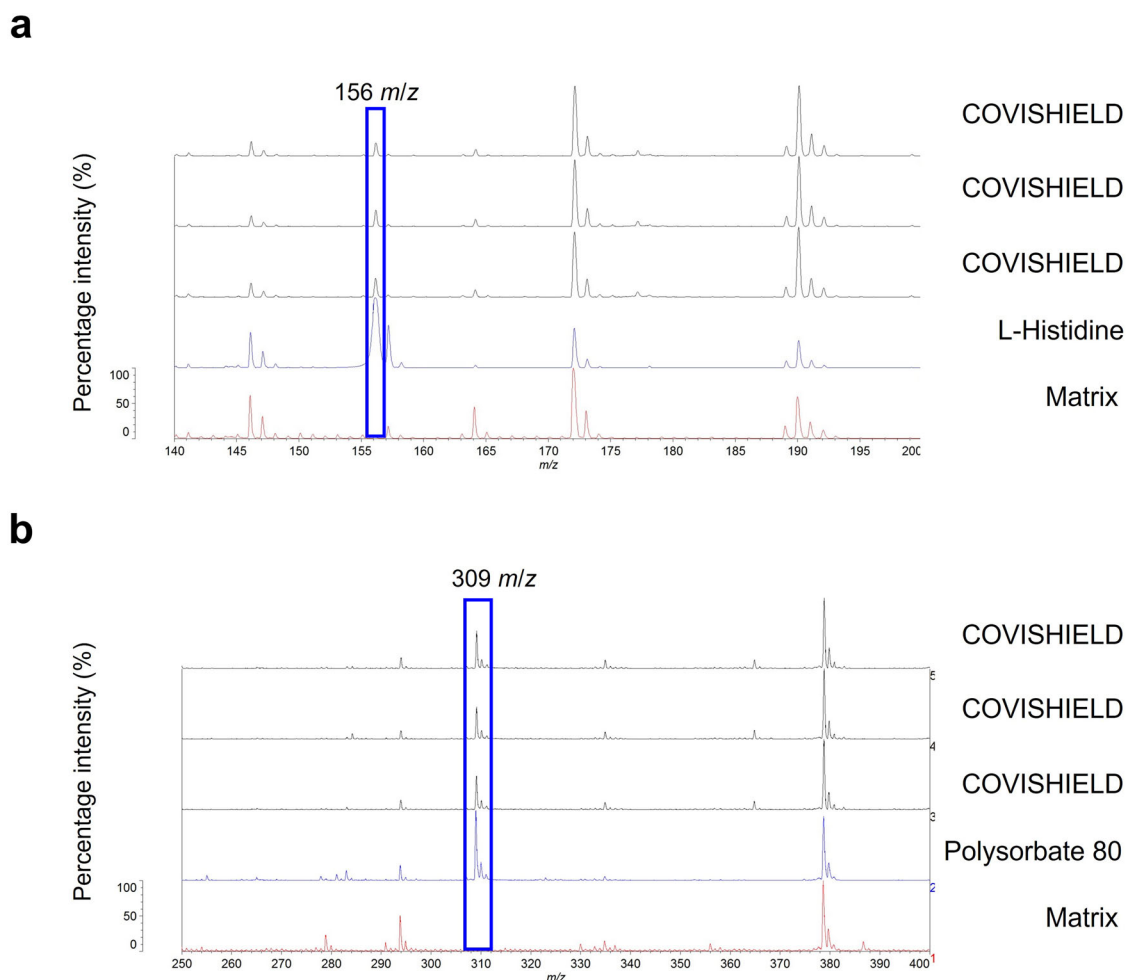


Fig. 3 | Identification of COVISHIELD™ COVID-19 vaccine constituents at 0–900 *m/z* using the Vitek-MS. **a L-histidine was identified at 156 *m/z*. **b** A low mass peak of polysorbate 80 was detected at 309 *m/z*. The COVISHIELD™ spectra from**

three different vials of vaccine batch 4122Z001 are shown and compared to L-histidine, polysorbate 80 and matrix spectra.

the mid-mass (700–2500 *m/z*) and high-mass (2000–20,000 *m/z*) ranges (Supplementary Fig. 7).

Analysis of vaccine vial labels

We investigated proof-of-concept that MALDI-ToF MS analysis could also be used to identify differences in chemical composition between vaccine vial label extracts from genuine COVISHIELD™ labels and an office stationery label (Fig. 9). The spectra for genuine COVISHIELD™ labels was found to be remarkably different to the office stationery label and differences could easily be identified simply by visualising the spectra (Fig. 9a) and without needing to perform any statistical analysis of the spectral data. In addition, PCA (Fig. 9b) and PLS-DA (Fig. 9c) scores plots of the genuine and stationery label spectra showed clear separation with no overlap of the 95% confidence regions and significant cross-validation and permutation results (Fig. 9d, e). This was confirmed by external validation which demonstrated that the PLS-DA model was able to distinguish between vaccine labels with 100% accuracy in the training and test sets using a 90/10 split (Supplementary Table 3). In addition to this 90/10 split, a 70/30 split was also carried out also showing perfect accuracy for the genuine labels (data not shown). When comparing between peaks of genuine COVISHIELD™ label and office stationery label, t-test statistical analysis revealed a total number of 395 significant ($p < 0.05$) peaks with the peak at 534 *m/z* as the variable of importance in projection with the highest score based on PLS-DA analysis, shown as the base peak for office stationery label (Fig. 9a). PCA could further distinguish between labels used in different batches of COVISHIELD™ vials

produced in Hadapsar and Manjari factories, although some overlapping of the 95% confidence regions were observed (Fig. 10a). In addition, this was supported by a robust PLS-DA model, shown by high accuracy, R2, and Q2 scores and a significant permutation test (Fig. 10b–d) with perfect accuracy of the model on the training and test data sets using a 90/10 split (Supplementary Table 4). In addition to this 90/10 split, a 70/30 split was also carried out also showing perfect accuracy for the different manufacturing sites (data not shown).

Discussion

The lack of established quality assurance systems within the complicated meshwork of global medicinal product supply chains puts the world at risk of surges in SF medicines and vaccines². This highlights the critical role of medicine regulatory authorities to prevent, detect and remove SF medicinal products at different points in the supply chain²⁴ and such monitoring should be an intrinsic part of disease surveillance programs to safeguard public health²⁵.

MALDI-ToF MS instruments measure the mass-to-charge ratio (*m/z*) of individual analyte ions and can be used for the analysis of complex mixtures with minimal sample preparation and rapid turnaround (data for each sample is acquired in only a few seconds)²⁶. Crucially, thousands of these MS instruments are widely available²⁷ in hospital microbiology laboratories globally, for bacterial identification, and therefore provide a potential accessible analytical network for local vaccine analysis. Although the MALDI-ToF instruments used in hospitals are of low resolution in comparison to other mass spectrometers, they were capable of differentiating

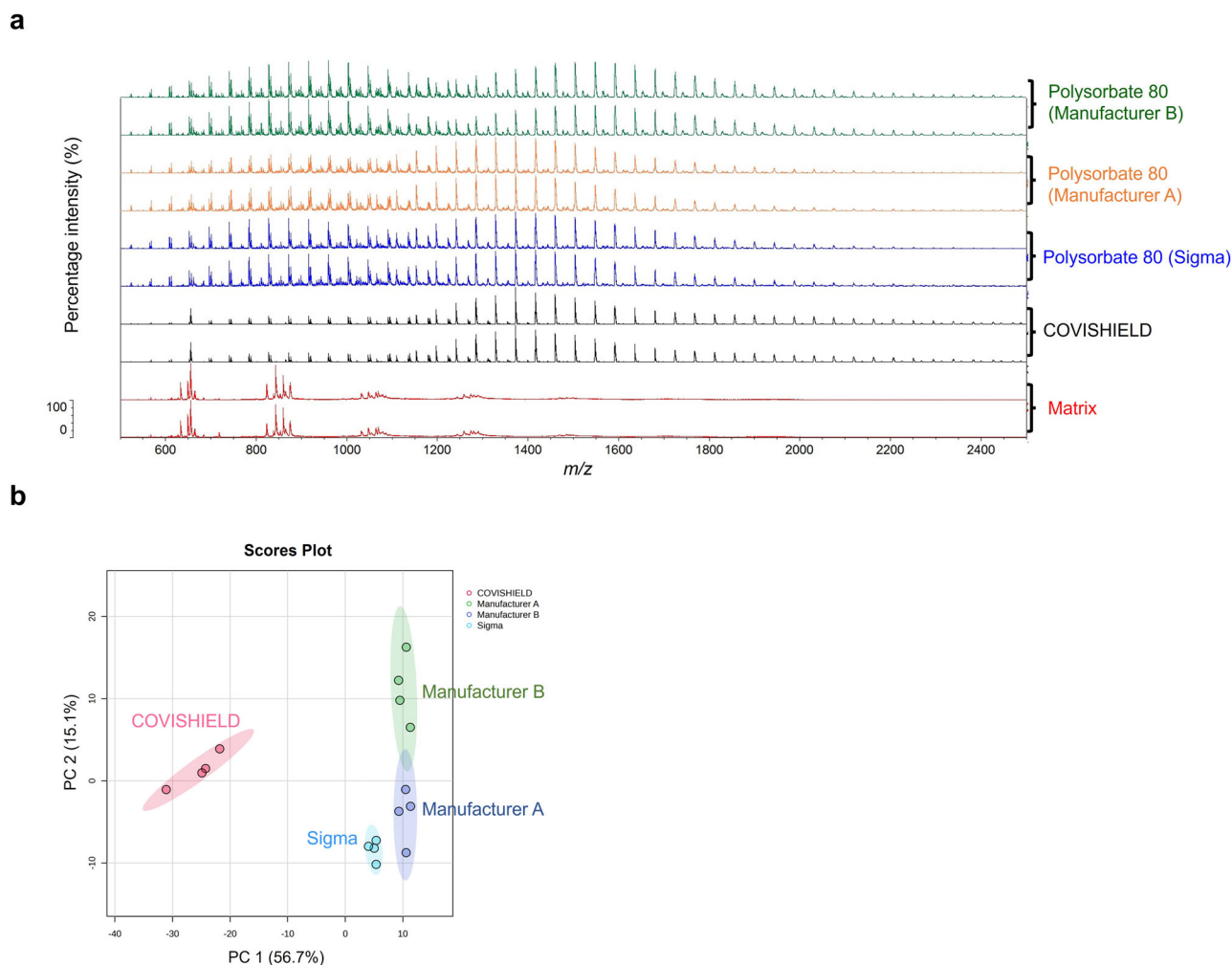


Fig. 4 | Vitek-MS spectra comparison between COVISHIELD™ and polysorbate 80 from three different manufacturers. **a** Spectra over the 500–2,500 m/z mass range showing different profiles of polysorbate 80 with the most dominant evenly spaced peaks between 600 and 2200 m/z . **b** PCA scores plot showing the distinct

grouping of COVISHIELD™ and polysorbate 80 from three different manufacturers. Samples were run with four technical replicates for each and only two representative spectra are shown.

genuine vaccines from all falsified vaccine surrogates tested and genuine labels from an office stationery label. A limitation of some MALDI-ToF instruments in hospitals is that only the 2000–20,000 m/z range is routinely used in microbial identification. Although this is a limited range, it does cover the mass range for the polysorbate 80 observed in this study (Supplementary Fig. 2b). Peaks such as histidine at 156 m/z and polysorbate 80 at 309 m/z (Fig. 3) would not be observed if only the routinely used mass range of 2000–20,000 m/z is used. However, many MALDI-ToF mass spectrometers in hospitals are already capable of analysing a wide mass range (0–500 m/z) covering these peaks and all other instruments set to analyse the 2000–20,000 m/z can be upgraded to analyse the wide mass range.

We demonstrate how MALDI-ToF MS with machine learning analysis of the results can be used to verify genuine vaccine vial labels and detect key excipients in the COVISHIELD™ vaccine and use them as indicators of the genuine vaccine. In addition, we confirmed that the PLS-DA model was robust, suggesting it could be used to predict new, previously uninvestigated vaccine samples, irrespective of origin, and confirm if it is a genuine or falsified vaccine as shown by the high accuracy of the external validation results in both training and test sets (Supplementary Table 1).

Falsified COVISHIELD™ vaccine and vial labels have been identified in Uganda, India and Myanmar²³. Since labels on the COVISHIELD™ vials have been falsified, we compared the extracts of a self-adhesive office label with the genuine COVISHIELD™ labels. MALDI-ToF MS analysis of label extracts with their adhesives showed that COVISHIELD™ vaccine labels had

distinct spectral profiles (Fig. 9a). PCA scores plot showed distinct clustered groups for the genuine labels, office stationery label and matrix background (Fig. 9b). In addition, a significant (permutation test p -value < 0.05) PLS-DA model was generated (Fig. 9c) that was able to distinguish between label types with 100% accuracy in the test set (Supplementary Table 3). A limitation is that it was not possible to obtain the actual falsified COVISHIELD™ vaccine label. From the photos published on the WHO alert²³, it appears as though the criminals used an office label on the falsified COVISHIELD™ vaccine vials and printed the text on the label using an office printer. Therefore, an office stationery label was similar to what had been used on the falsified vaccine vials. While the label tested was not an actual falsified label, the data shows that MALDI-ToF is capable of non-invasively detecting falsified vaccines. The spectra of only one office label were analysed for proof-of-concept. Although only one office label was compared to several genuine COVISHIELD™ labels, the permutation test confirms that the separation observed is unlikely to have resulted by chance.

Different score plots were observed between the two manufacturing sites (Fig. 10), inferring the possibility of either slightly different label materials/adhesives between factories or that the same materials/adhesives were used but MALDI-ToF MS is sensitive enough to detect a different batch of label material or adhesive. Since MALDI-ToF was able to differentiate genuine labels from the Hadapsar and Manjari factories (possibly due to a different batch of adhesive/label), it would be able to differentiate a genuine label and any non-genuine label used by criminals. We have also analysed the

Table 2 | The falsified vaccine surrogates used for MALDI-ToF MS analysis

| Vaccine surrogates | Manufacturer | Batch/part number | Composition | Remarks |
|------------------------------------|---|-------------------|---|--|
| 0.9% w/v sodium chloride injection | Demo S.A Pharmaceutical Industry | 24598/0002 | 0.9% w/v NaCl in water for injection | Surrogate for falsified COVID-19 vaccines intercepted in China and India (Mumbai) ⁸ |
| 5.0% w/v D-glucose | B/Braun | 03551/0059 | D-glucose 5.0% w/v Glucose solution prepared in distilled water | Surrogate for falsified COVID-19 vaccines intercepted in the Philippines ⁹ |
| Amikacin, 250 mg/ml | Hospira (Used for the Sirius Biolyter) | 05015997122159 | 250 mg/ml amikacin sulphate, sodium citrate, sodium metabisulphite and water for injection | Surrogate for falsified COVID-19 vaccines intercepted in India ^{10,34} |
| Gentamicin, 40 mg/ml | MA Holder Tillomed Laboratories Ltd. (used for the bioMérieux Vitek-MS) | 11311/0604 | 250 mg/ml amikacin sulphate, sodium metabisulphite, dihydrate, sulfuric acid and water for injection | |
| Hyaluronic acid | Demo S.A. | 05208063001339 | 40 mg/ml gentamicin sulphate, 1.60 mg/ml sodium metabisulphite, disodium edetate | Surrogate for falsified non-COVID vaccines intercepted in Indonesia ⁸ |
| Tap water | Guangzhou Ailian Cosmetic Co Ltd. | QB/T 2660 | Anti-wrinkle serum containing water, glycerine, propylene glycol, methylisothiazolinone, bis(hydroxymethyl)imidazolidinyl urea, iodopropynyl butylcarbamate, disodium EDTA, xanthan gum, sodium hyaluronate | Surrogate for falsified COVID-19 vaccines intercepted in Poland ^{4,1} (the precise formulation and form of intercepted hyaluronic product unknown apart from it being reported being an anti-wrinkle formulation) |
| Milli-Q water | Biochemistry/Chemistry Research Laboratory, Oxford | N/A | Tap water | Tap water from the building water facility |
| Water for injection | Merck Millipore | N/A | Water from a Milli-Q Direct 8 water purification system | Purified double-distilled water |
| | Demo S.A Pharmaceutical Industry | 24598/001 | Sterile water for preparation of a medicine intended for injection or infusion | Water for injection in plastic ampoules |

label extracts of other COVID-19 vaccines (data not shown due to non-disclosure agreements in place) which showed unique spectra, different to the genuine COVISHIELD™ label, indicating that vaccine labels from different vaccine manufacturers have their own mass spectral fingerprints which could be used to non-invasively check authenticity. The criminal reuse of genuine vials filled with non-vaccine liquids would not be detected. However, these results illustrate a promising additional non-invasive method to detect falsification of vaccines and the approach could be applied to analyse the labels or packaging of all medicines as well as other items known to be falsified (e.g. perfume bottles). In this study, MALDI-ToF MS was found to be capable of detecting even differences in the batches of adhesive used between the Manjari and Hadapsar sites (Fig. 10). Although the spectra were different, the dominant peaks were the same suggesting that the difference is due to a different batch of adhesive/label (Fig. 10e). These dominant peaks could be included in a reference spectral library to test for authenticity. In addition, there are less intense peaks which vary between batches and can help to confirm if a spectrum matches with that of a reference label from the same batch. While it is required for vaccine manufacturers to disclose the list of excipients in vaccines, details for the label are proprietary information making it almost impossible for criminals to reproduce a label with identical MALDI-ToF MS spectra without knowing the label material, label manufacturer and the exact composition (formulation) of the adhesive. Furthermore, they would need to know the precise concentration of ingredients used in the specific adhesive batch they are attempting to copy since the technique was sensitive enough to differentiate between adhesive batches (Fig. 10). Many vaccine manufacturers also have security features on vaccine labels which are difficult to replicate but the unique MALDI-ToF spectra of the label extracts (molecular fingerprints) add a considerably higher level of security that cannot be replicated by falsifiers. If a vaccine manufacturer changes the label or its adhesive, a label from a genuine batch could be used as a reference to compare to a test label. The advantage of analysing the label is that it is non-invasive and the vials can be retained in the supply chain. However, where a vaccine fails the label check and remains suspect, the vaccine liquid should be additionally analysed.

MALDI-ToF MS can also be utilised to establish a molecular profile for a vaccine^{20,21}. Vaccine constituents such as polysorbate 80 (with evenly spaced peaks mainly between 500-2500 *m/z*) and L-histidine (at 156 *m/z* corresponding to [histidine + H]⁺) are known to be seen by positive ionisation mass spectrometry^{28,29} and their presence was confirmed in the COVISHIELD™ vaccine using authentic standards. Peaks corresponding to L-histidine (Fig. 3a) and polysorbate 80 (Figs. 3b and 4) are therefore possible markers of the COVISHIELD™ vaccine. We expect that the 309 *m/z* peak, unique to the authentic COVISHIELD™ vaccine, could be the C18:1 ester of polysorbate as previously reported³⁰.

Polysorbate 80 consists of a population of ethoxylated structures with different masses observed in MALDI-ToF MS spectra as evenly distributed peaks resulting from random polymerisation. The peaks are spaced apart in the spectra by 44 Da, equal to the mass of ethylene oxide (C₂H₄O; 44.05 g/mol). These evenly spaced peaks were observed predominantly between 500-2500 *m/z* (Fig. 4a and Supplementary Fig. 7). We analysed polysorbate 80 from multiple sources; a chemical supplier (Sigma) and two different online stores. The PCA analysis on spectra profiles was able to distinguish between polysorbate 80 from each manufacturer (Fig. 4b), suggesting that the distribution of polysorbate 80 peaks in the COVISHIELD™ vaccine could act as an internal marker for authenticity screening. While this study has focused on COVISHIELD™, a very large number of medicines contain polysorbates and therefore may be a good internal marker for authenticity. For example, COVID-19 (Paxlovid; nirmatrelvir-ritonavir)³¹, anti-malarial (Riamet; artemether-lumefantrine)³², and cholesterol-lowering (Lipitor; atorvastatin)³³ drugs all contain polysorbate 80 and all have been associated with falsified products, the latter of which saw the largest recall of falsified medicines in the US³³. The method could also be applied to drugs containing other polysorbates, such as polysorbate 20 and potentially for analysing other polymers commonly used as excipients in vaccines such as PEGylated lipids (e.g. polyethylene glycol 2000 dimyristoyl glycerol in Spikevax®

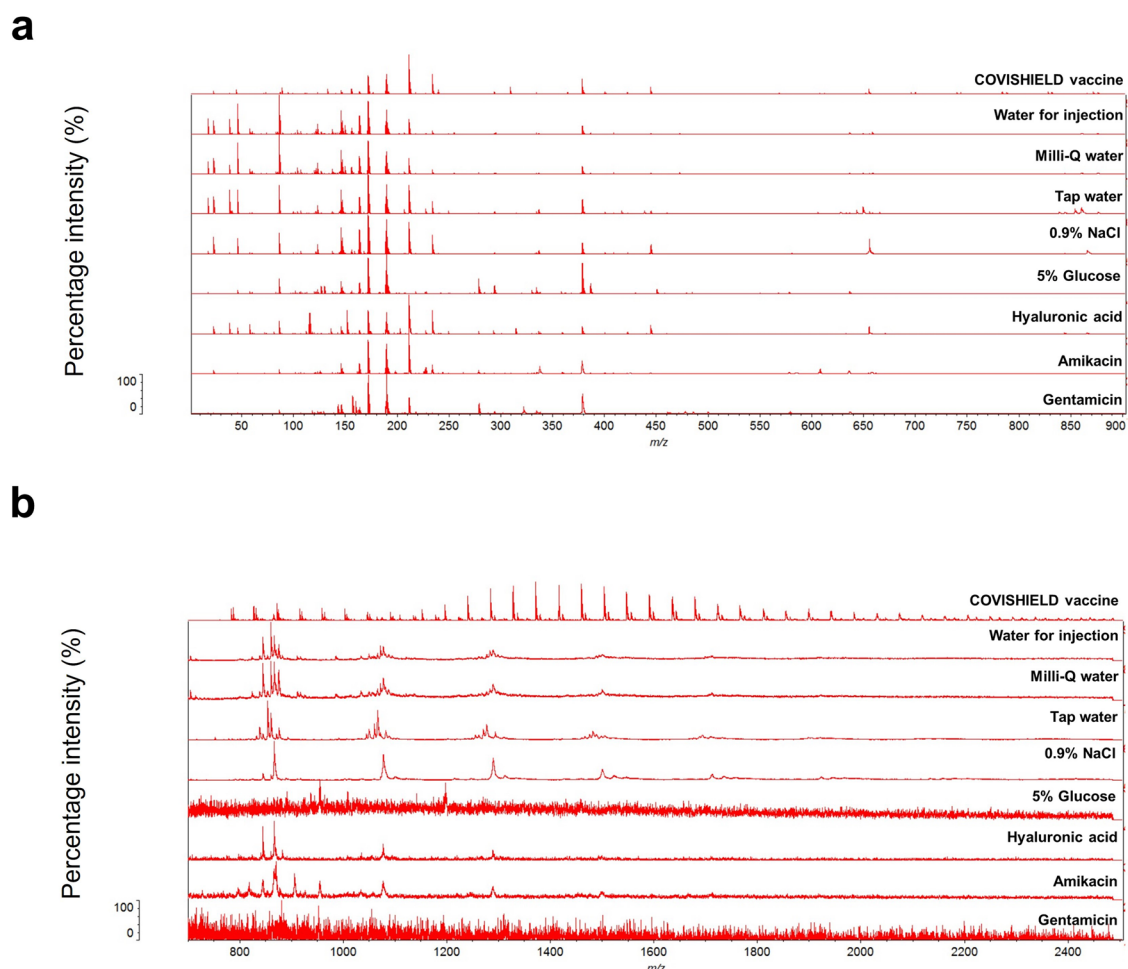


Fig. 5 | Vitek-MS spectra for the COVISHIELD™ vaccine and eight falsified vaccine surrogates. Spectra were generated at (a) 0–900 m/z and (b) 700–2500 m/z mass ranges.

COVID-19 vaccine, Moderna) or Triton X surfactants (e.g. octoxinol-9 in Quadrivalent Influenza vaccine, Sanofi).

As expected, MALDI-ToF MS was not able to detect the most dominant excipient sucrose since it is not usually seen with positive ionisation mass spectrometry. Also, as expected, ethanol in the vaccine was not visible since it evaporated off the MALDI target. Both sucrose and ethanol are excipients that we had previously detected using SORS by scanning unopened COVISHIELD¹⁷. However, SORS did not detect polysorbate 80 or L-histidine, highlighting the complementarity of the two techniques where SORS could be used as a screening technique and MALDI-ToF as a confirmatory analysis where an anomaly is identified.

MALDI-ToF MS of vaccines from vials of the same batch (intra-batch), different batches (inter-batch) and different manufacturing sites showed similar spectra with the same relative intensities among the excipient peaks for histidine and polysorbate 80. Therefore, falsified vaccines containing the same excipients but at different relative concentrations could be identified since the relative intensities among the histidine and polysorbate 80 peaks in falsified vaccines would differ from the relative intensities consistently observed with the genuine vaccine. If concentrations of histidine and polysorbate 80 were identical then differentiation may not be possible using only relative peak intensity ratios. In this case, the fingerprint of polysorbate 80, which we show is unique for a chemical manufacturer, would also need to be analysed. Furthermore, the PCA analysis yielded no significant differences in both intra- and inter-batch analyses (Fig. 2), reflecting the standard manufacturing quality implemented in both factories. MALDI-ToF and PCA analysis could distinguish COVISHIELD™ vaccine from the falsified vaccine surrogates (Fig. 6a), which strongly suggests that they could be used to detect falsified vaccines in risk-based post-market surveillance. In

addition, the dendrogram classification grouped COVISHIELD™ samples into a monophyletic group separated from other surrogates (Fig. 7).

Substandard quality of a medicinal product may be generated from errors, negligence, or poor practice in manufacturing, procurement, regulation, transportation, or storage⁷. One of the potential risks in vaccine supply chains is the possibility of temperature excursions during transportation, or failure in maintaining the cold storage (cold chain) conditions, especially in countries where the ambient temperature is high. We therefore investigated the effect of freeze-thaw cycles and heat exposure on the spectra of the vaccine. Although the test set performed well (Supplementary Table 2), the high accuracy observed is likely due to chance and multivariate analysis was not able to detect any significant changes in heat-exposed samples (Fig. 8).

MALDI-ToF was unable to detect or check the stability of the active constituent of the vaccine and thus other methods (e.g. viral vector virus titration) are needed for this purpose. Although MALDI-ToF MS could not identify the active ingredients in the vaccine, it was still able to discriminate between simulated falsified vaccines and the genuine comparator vaccine. To detect active ingredients, we have recently proposed and evaluated repurposing rapid diagnostic tests (RDTs)¹⁸. This highlights the complementarity of both MALDI-ToF and RDTs to confirm if a vaccine is genuine or falsified. MALDI-ToF has the advantage of its distribution in most reference hospitals and many microbiology laboratories in the world, including in some LMIC, and therefore the technique is deployable in the field. Since thousands of MALDI-ToF mass spectrometers are in hospitals around the world, the vaccines could potentially be tested prior to vaccine administration in the same hospital.

Limitations of the study include that we did not have access to collected falsified vaccines. According to online news websites, the falsified COVISHIELD™ vaccine was found in a vaccination camp in Kolkata, India, where

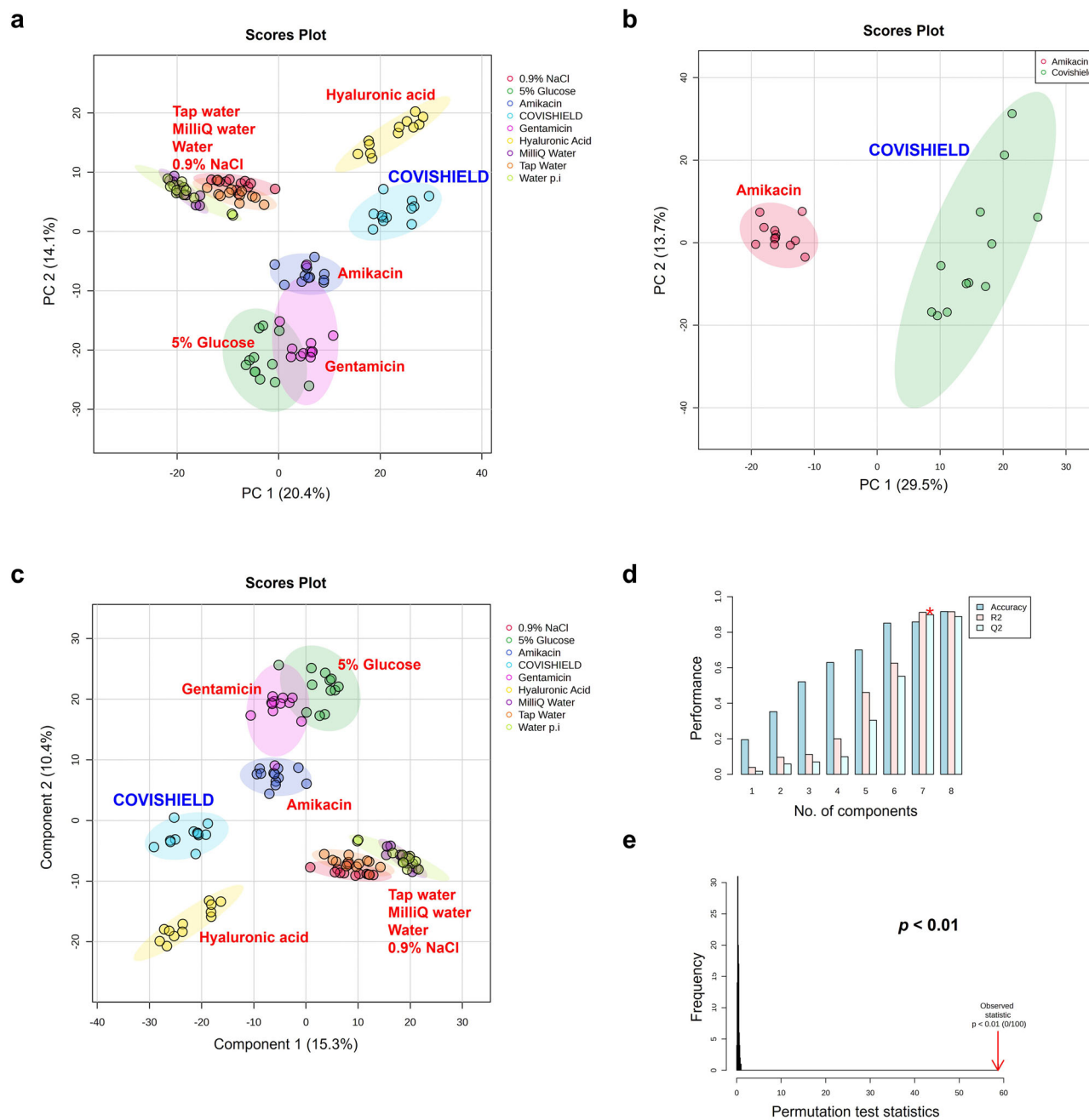


Fig. 6 | Multivariate statistical analyses of the MALDI-ToF MS spectra generated from genuine COVISHIELD™ COVID-19 vaccine samples and eight common falsified vaccine surrogates. PCA score plots were generated from analysis of Vitek-MS peak list data over the 0-900 m/z mass range ($n = 3$ with four technical replicates for

each n) for (a) COVISHIELD™ vaccine as compared to eight common falsified vaccine constituents and (b) COVISHIELD™ compared to Amikacin only, along with (c) PLS-DA score plot, d PLS-DA cross-validation results, and e PLS-DA permutation analysis. The elliptical area reflects the region within 95% confidence interval of the measurement.

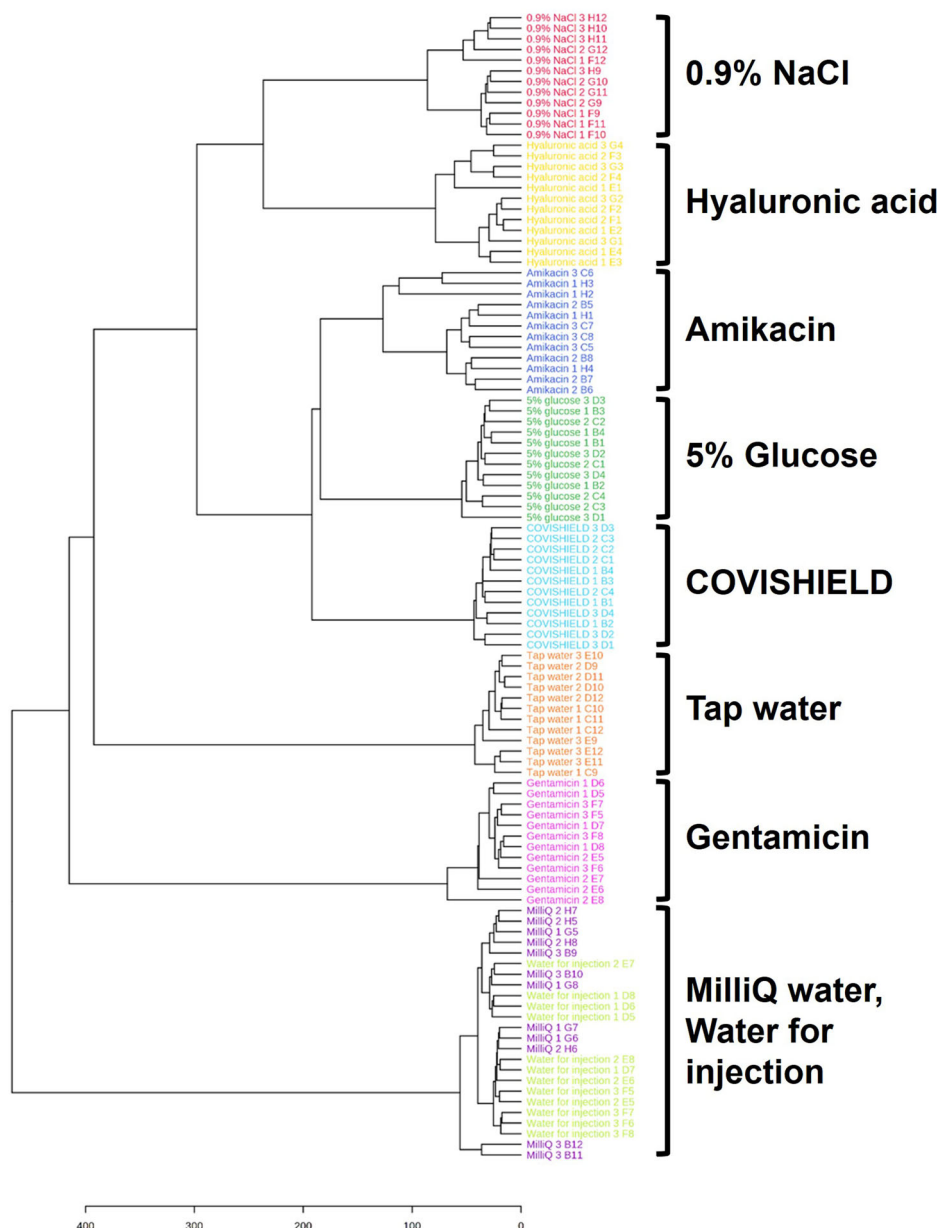
amikacin was used³⁴. Using our approach, amikacin could be readily differentiated from the genuine COVISHIELD™ vaccine (Fig. 6b). Dilution of genuine vaccines is far less likely to be carried out by criminals since they would need to obtain the genuine vaccine to do this. We are not aware of any case where vaccines have been falsified by dilution and therefore have not tested this with COVISHIELD™.

As part of a future project, custom spectral libraries for genuine vaccines will be generated which could be distributed to international medicine regulatory agencies to use on MALDI instruments in their respective countries. Since no batch-to-batch variation was detected for the COVISHIELD™ vaccine (Fig. 2), a fixed spectral library could be used. Since differences were observed in the label spectra between manufacturing sites, a reference spectra would need to be generated

from the label of a known genuine batch and then compared to a suspect label. Close liaison would be needed between vaccine manufacturers and regulatory authorities to ensure timely notification of changes in vaccine and label constituents.

In conclusion, we have demonstrated that MALDI-ToF MS spectral analysis combined with machine learning and multivariate analysis could be used for authenticating a COVID-19 vaccine. Excellent inter-batch reproducibility was observed for the COVISHIELD™ vaccine among six different batches and across two different manufacturing sites. Two excipients (L-histidine and polysorbate 80) in the COVISHIELD™ vaccine could be successfully detected and the spectra were easily differentiated, both visually and using multivariate analysis, from falsified vaccine surrogates. In addition, while analysis of the

Fig. 7 | Dendrogram analysis of the MALDI-ToF MS spectra ($n = 3$, with four technical replicates for each n) for the COVISHIELD™ vaccine as compared to eight surrogates of falsified vaccine constituents. This classification is based on data from the Vitek-MS instrument at 0-900 m/z .



vaccine is destructive, we showed that the analysis of vaccine vial labels has the potential for use as a non-invasive method in vaccine authentication and could be applied to other medicine labels. Since label analysis is non-invasive, it would allow the tested vaccine vials to be retained in the supply chain post-screening.

Methods

Vaccine samples

A total of 45 vials of genuine Serum Institute India (SII) COVISHIELD™ COVID-19 vaccine, hereafter mentioned as COVISHIELD™ vaccine, were received for the study. The vials were acquired from five production batches at the Hadapsar factory (Batch 1-5) and the Manjari factory (Batch 6), both located in Pune, Maharashtra, India (Fig. 1 and Table 1). Three vials per batch were used for batch-to-batch analysis by MALDI-ToF MS with four technical replicates (a total of 12 replicates per batch).

The COVISHIELD™ vaccine is reported to contain the excipients L-histidine, L-histidine hydrochloride monohydrate, magnesium chloride hexahydrate, polysorbate 80, ethanol, sucrose, sodium chloride, and disodium edetate dihydrate (EDTA)³⁵.

Vaccine samples were shipped in a temperature-controlled container and stored at 2-8°C upon arrival, according to the manufacturer’s recommendation, and kept on ice prior to spotting on the MALDI targets. All samples were analysed within their date of expiry.

Single solutions of ionisable excipients

For the comparative vaccine excipient measurements, the following solutions were used: L-histidine in water (<15 mM; Sigma-Aldrich) and polysorbate 80 in water (<1% w/v Tween 80; Sigma-Aldrich). Commercially-available polysorbate 80 from two different online markets (www.thesoapery.co.uk, referred to as manufacturer A and www.cosmeticsmadeeasy.com, referred to as manufacturer B) were also prepared in the same <1% w/v concentration. Although not necessarily identical, these were in the same concentrations as those used in the authentic vaccines.

Surrogate of falsified vaccines

We did not have access to falsified vaccine samples seized in supply chains. Hence, to assess the capability of the techniques to detect falsified COVID-19 vaccine products, surrogates for potential and actually intercepted

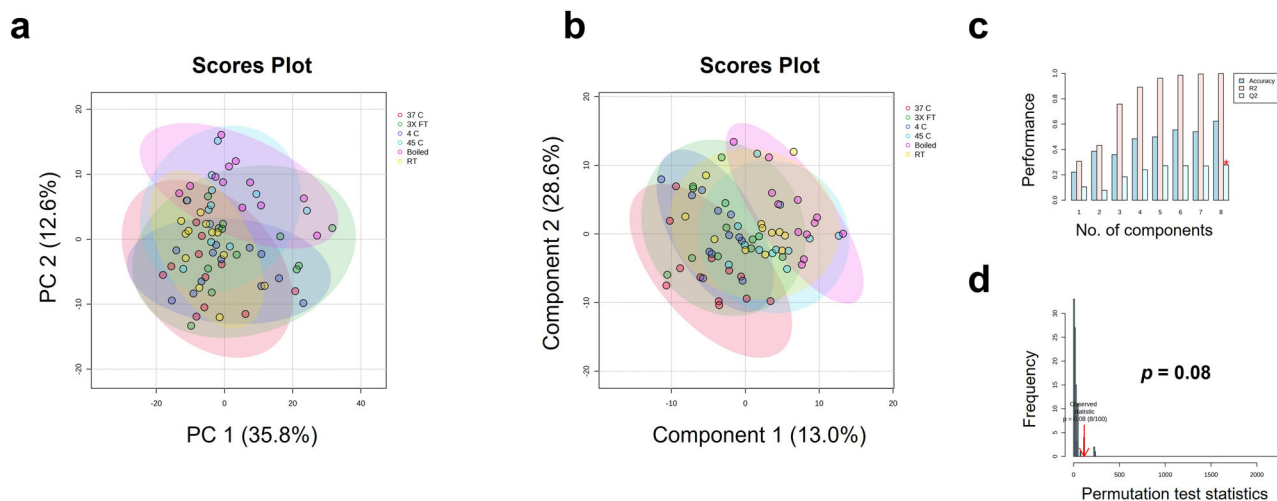


Fig. 8 | Vitek-MS analysis at 0-900 *m/z* comparing COVISHIELD™ vaccine vials exposed to freeze thaw cycles and different temperature conditions (three vials run (*n* = 3), with four technical replicates for each *n*). **a** PCA score plot, **b** PLS-DA score plot, **c** PLS-DA cross-validation results, and **d** PLS-DA permutation analysis.

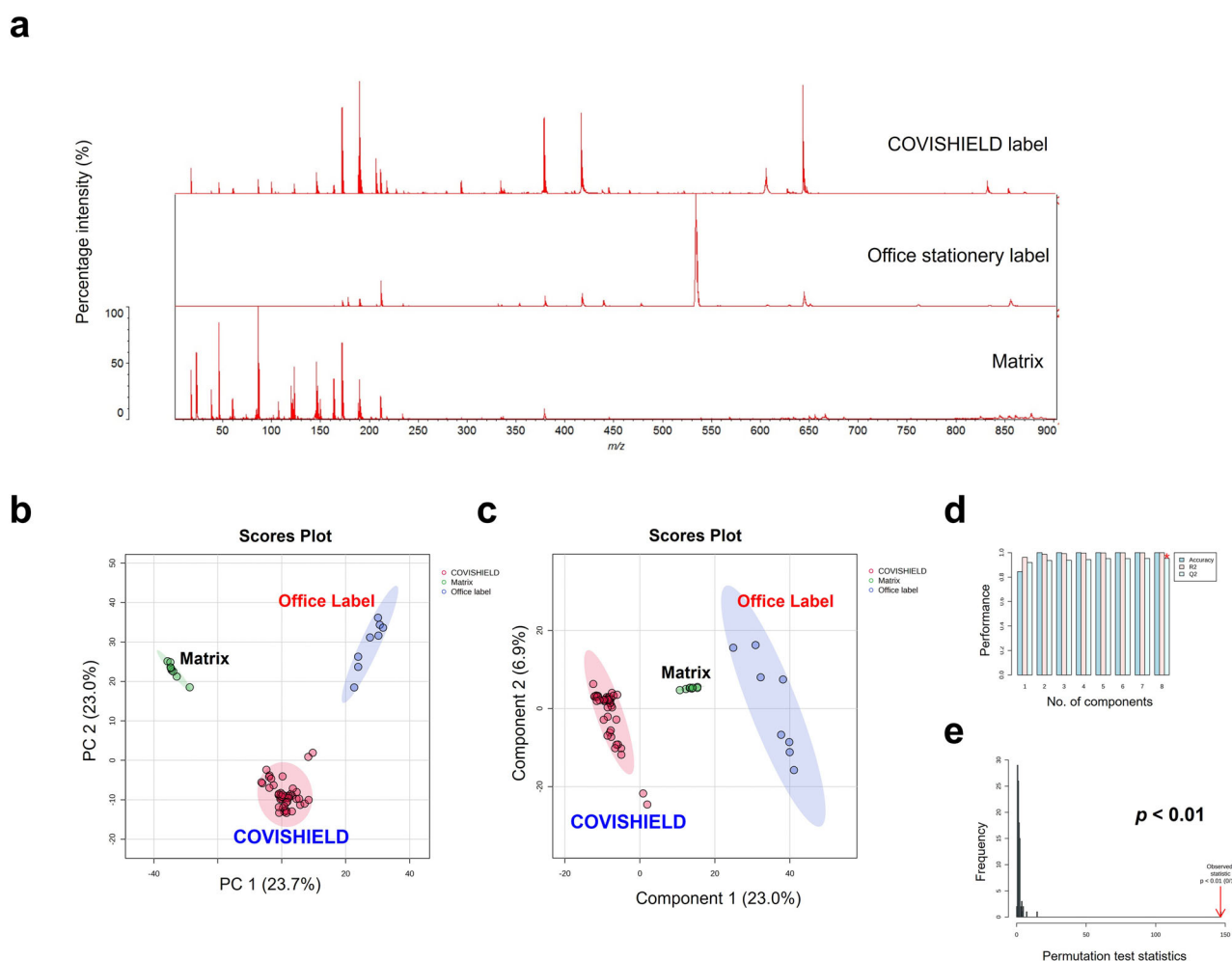


Fig. 9 | Vitek-MS analysis of labels over the 0-900 *m/z* mass range comparing COVISHIELD™ label extracts from six batches (*n* = 6), an office stationery label (*n* = 2), and the CHCA matrix as a background control (*n* = 1), with four technical replicates for each *n*. **a** The 0–900 *m/z* representative spectra of label extracts and matrix, **b** multi-variate analysis PCA score plot, **c** PLS-DA score plot, **d** PLS-DA cross-validation results, and **e** PLS-DA permutation analysis.

falsified products were used (Table 2). Falsified vaccine constituents were identified from reports available in the public domain, both in the scientific and lay literature⁸.

MALDI-ToF MS processing of samples

Sample processing was performed in three biological replicates (*n* = 3) with four technical replicates for each *n*. Samples were spotted onto disposable

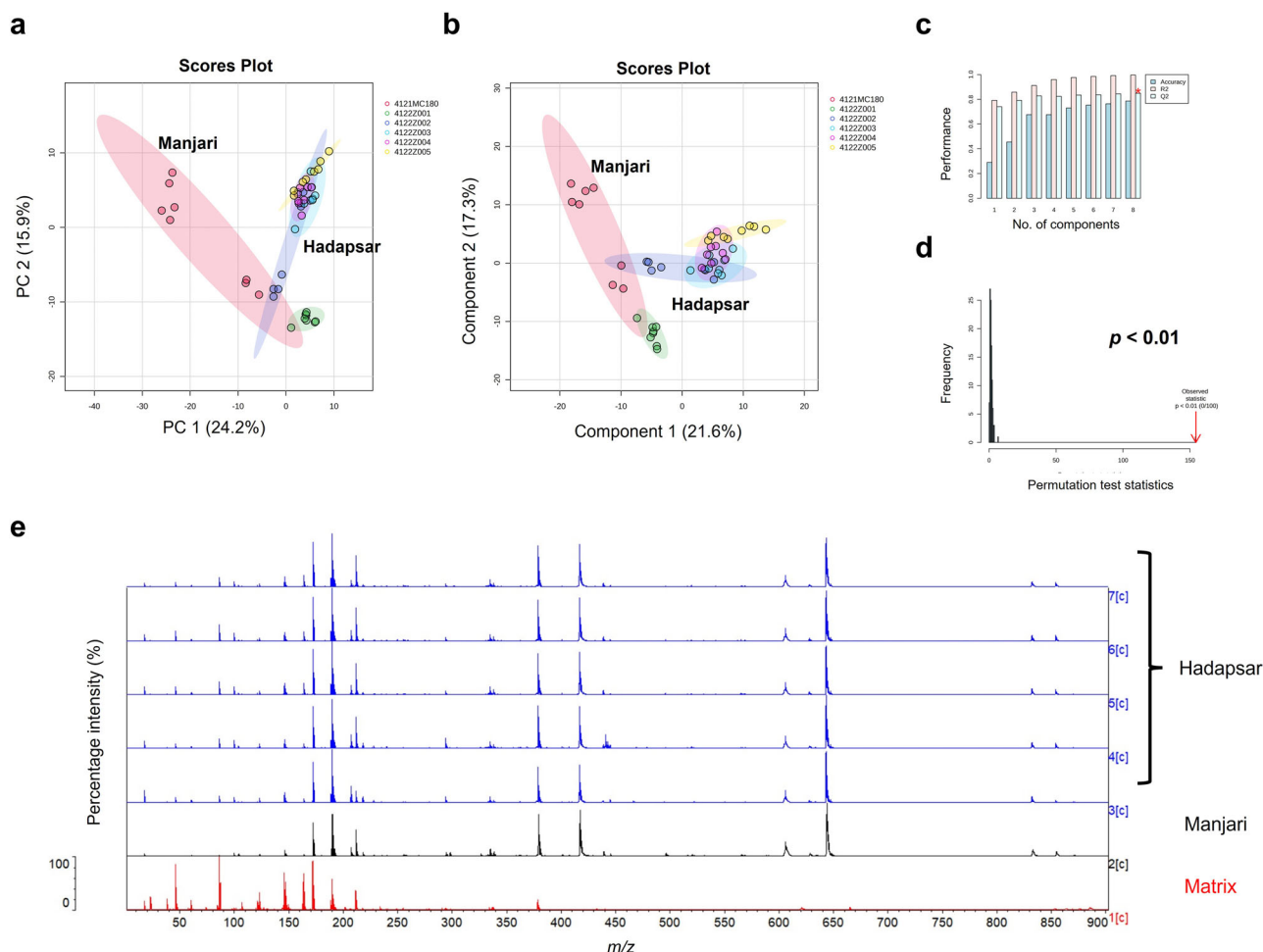


Fig. 10 | Vitek-MS analysis over the 0–900 *m/z* mass range of COVIDSHIELD™ vial label extracts from six different batches (*n* = 8 technical replicates per batch) manufactured in Hadapsar and Manjari factories (Table 1). **a** PCA score plot, **b** PLS-DA score plot, **c** PLS-DA cross-validation results, **d** PLS-DA permutation analysis, and **e** the 0–900 *m/z* representative spectra of label extracts from Hadapsar (five different batches) and Manjari (one batch), compared to matrix.

MALDI target plates (Vitek-MS P/N 410893 and Biotyper® Sirius P/N 1840375) compatible with VITEK® MS (bioMérieux), ‘Vitek-MS’, and Biotyper Sirius (Bruker) MALDI-ToF MS, ‘Biotyper’, instruments. Each technical replicate spot was produced by mixing an equal volume of sample and alpha-cyano-4-hydroxy-cinnamic acid (CHCA) matrix (CHCA/HCCA, Vitek-MS CHCA; P/N 411071, Bruker MS-CHCA solvent P/N 900666 and matrix P/N 8255344) then pipetting 2 µL of the mixture onto each replicate spot of the target plate using an ASSIST PLUS pipetting robot (INTEGRA Biosciences Ltd, Berkshire, UK). The sample spots were allowed to air dry at room temperature. All samples used were within their expiry dates at the time of experimental work. The mass ranges analyzed were 0–900, 700–2500 and 2000–20,000 *m/z* using our previously described method²¹.

Degraded samples

To study the effect of temperature on the stability of the COVIDSHIELD™ vaccine, the following temperature conditions were investigated: vaccine vials stored at 4 °C (within the 2–8 °C manufacturer’s recommended storage condition) and vials stored at room temperature (recorded as 20 ± 1 °C) and at elevated temperature conditions of 37 °C, 45 °C and 100 °C (boiled). In addition, vials were exposed to three freeze-thawed cycles.

For each of these storage conditions, three unopened vials of COVIDSHIELD™ vaccine (*n* = 3, all from batch no. 4122Z001) were used. The 4 °C vials were refrigerated for 7 days, and the other vials were stored on bench at room temperature or in incubator ovens set at 37 or 45 °C for 7 days. The vials undergoing freeze-thaw cycles were frozen at –80 °C for 24 h and then

thawed at room temperature (20 °C) for 1 h. The freeze-thaw cycle was repeated twice more. The boiled vials were placed inside a beaker of boiling water on a 100 °C hot plate for 10 min. All samples were stored at 4 °C after undergoing the above temperature conditions.

Vaccine vial label analysis

A small piece of the vaccine vial label (approximately 2 × 2 mm) was cut, in duplicate, from different batches of the COVIDSHIELD™ vaccine vials (*n* = 3, with four technical replicates for each *n*). The self-adhesive office stationery labels (*n* = 2, with four technical replicates for each *n*) were used for comparison. Each piece of the label was then thoroughly mixed by vortexing, to help dissolve the adhesive into solution, with 10 µL of CHCA matrix, and then incubated for 10 min at room temperature. A volume of 2 µL of the extract was spotted in quadruplicate onto a MALDI plate and run to generate MS spectra at low mass (0–900 mass per charge, *m/z*), mid mass (700–2500 *m/z*) and high mass (2000–20,000 *m/z*) ranges²¹.

Data analysis

Raw spectra from both instruments were visually analyzed and plotted using Shimadzu LaunchPad (for Vitek-MS data) and Bruker FlexAnalysis (for Biotyper data) software. Vitek-MS raw data files were acquired in mzXML format using Shimadzu LaunchPad software. Bruker CompassXport was used to acquire Biotyper data. Spectra (four spectra from four technical replicates for each *N*) were analysed using a workflow that combined MALDI-ToF with open-source machine learning and statistical analysis²¹. Briefly, data exploration was performed using R statistical software v.4.1.3

using packages MALDIQuant³⁶, MALDIrppa, caret, lattice, factoextra, and dendextend while data visualisation was performed in MetaboAnalyst³⁷. The resulting peak list from MALDIQuant was then analyzed using the ‘Statistical Analysis (one factor)’ module of MetaboAnalyst online software. Experimental data were uploaded as peak intensities in ‘‘Samples in columns (unpaired)’’ format. Data filtering was performed using an interquartile range (IQR) statistical filter to identify and remove variables that are unlikely to be of use when modelling the data. The data were normalised by sum and scaled using pareto scaling (mean-centered and divided by the square root of the standard deviation of each variable). Unsupervised principal component analysis (PCA) and supervised multivariate analysis with machine learning algorithm partial least squares-discriminant analysis (PLS-DA) were used to model the data. The PLS-DA cross-validation (CV) was performed using 8 maximum components to search and 5-fold CV method, and permutation testing validation using the separation distance method and 100 permutation numbers³¹. Hierarchical dendrogram clustering was performed using Euclidean distance measure and Ward clustering algorithm methods.

PLS-DA external validation and confusion matrices

For each significant PLS-DA model generated, external validation was performed by randomly selecting 10% of the data to use as a pseudo external test set. Confusion matrices were produced as previously described³⁸. In brief, PLS-DA models were generated using either (1) the entire data set or (2) 90% of each class randomly selected as a training set which was then used to predict both the training and test sets. The accuracy of the PLS-DA predictions relative to the true classification of each sample is then summarised in confusion matrices using R code generated in-house³⁹ and the *ropls*⁴⁰ package.

Data availability

All data generated or analysed during this study are included in this published article and its supplementary information files.

Received: 25 March 2024; Accepted: 12 December 2024;

Published online: 30 January 2025

References

- Barouch, D. H. Covid-19 vaccines - immunity, variants, boosters. *N. Engl. J. Med.* **387**, 1011–1020 (2022).
- Newton, P. N. & Bond, K. C. COVID-19 and risks to the supply and quality of tests, drugs, and vaccines. *Lancet Glob. Health* **8**, e754–e755 (2020).
- Piranty, S. Coronavirus fuels a surge in fake medicines. *Coronavirus fuels a surge in fake medicines* <https://www.bbc.co.uk/news/health-52201077> (2020).
- Srivastava, K. Fake covid vaccines boost the black market for counterfeit medicines. *BMJ* **375**, n2754 (2021).
- World Health Organization. *WHO Global Surveillance and Monitoring System for Substandard and Falsified Medical Products*. (World Health Organization, Geneva, 2017).
- World Health Organization. Substandard and falsified medical products - Key facts. <https://www.who.int/news-room/fact-sheets/detail/substandard-and-falsified-medical-products> (2018).
- Newton, P. N., Bond, K. C. & Oxford Statement signatories. Global access to quality-assured medical products: the Oxford Statement and call to action. *Lancet Glob. Health* **7**, e1609–e1611 (2019).
- Medicine Quality Research Group, University of Oxford. Medical Product Quality Report – COVID-19 Issues. Issue 15, January, February & March 2022. https://www.iddo.org/sites/default/files/publication/2022-09/Medical%20Product%20Quality%20Report_Covid-19_Issue15_January-March2022_V1.1.pdf (2022).
- Gupta, S. & Yeung, J. Thousands thought they were getting the Covid vaccine. They were injected with salt water instead. <https://edition.cnn.com/2021/07/05/india/india-fake-covid-vaccine-scam-intl-hnk/index.html> (2021).
- Kaur, B. *Officials seize large cache of fake COVID vaccines, drugs, test kits in Varanasi*. The Wire <https://science.thewire.in/health/up-fda-officials-seize-fake-covid-vaccines-drugs-test-kits-varanasi/> (2022).
- Hindustan Times. *People may have got antibiotics at fake jab camp in Kolkata: Cops*. Hindustan Times <https://www.hindustantimes.com/india-news/people-may-have-got-antibiotics-at-fake-jab-camp-in-kolkata-cops-101624561190596.html> (2021).
- World Health Organization. *Medical Product Alert N°7/2021: Falsified COVID-19 Vaccine AstraZeneca*. WHO. <https://www.who.int/news/item/04-11-2021-medical-product-alert-n-7-2021-falsified-covid-19-vaccine-astrazeneca> (2021).
- BBC. *Coronavirus: Pfizer confirms fake versions of vaccine in Poland and Mexico*. BBC <https://www.bbc.co.uk/news/world-56844149> (2021).
- World Health Organization. *Medical Product Alert N°6/2021: Falsified Pfizer-BioNTech COVID-19 Vaccine*. WHO <https://www.who.int/news/item/04-11-2021-medical-product-alert-n-6-2021-falsified-pfizer-biontech-covid-19-vaccine> (2021).
- World Health Organization. Full List of WHO Medical Product Alerts. <https://www.who.int/teams/regulation-prequalification/incidents-and-SF/full-list-of-who-medical-product-alerts> (2024).
- Assi, S., Arafat, B., Abbas, I. & Evans, K. Evaluation of portable near-infrared spectroscopy for authentication of mRNA based COVID-19 vaccines. *PLoS One* **17**, e0267214 (2022).
- Mosca, S. et al. Innovative method for rapid detection of falsified COVID-19 vaccines through unopened vials using handheld Spatially Offset Raman Spectroscopy (SORS). *Vaccine* **41**, 6960–6968 (2023).
- Bharucha, T. et al. Repurposing rapid diagnostic tests to detect falsified vaccines in supply chains. *Vaccine* S0264-410X(24)00019–7 <https://doi.org/10.1016/j.vaccine.2024.01.019> (2024).
- Tsuchida, S., Umemura, H. & Nakayama, T. Current status of matrix-assisted laser desorption/ionization-time-of-flight mass spectrometry (MALDI-TOF MS) in clinical diagnostic microbiology. *Molecules* **25**, E4775 (2020).
- García-Cañas, V. et al. Approach to the profiling and characterization of influenza vaccine constituents by the combined use of size-exclusion chromatography, gel electrophoresis and mass spectrometry. *Biol. J. Int. Assoc. Biol. Stand.* **38**, 294–302 (2010).
- Clarke, R. et al. Using matrix assisted laser desorption ionisation mass spectrometry combined with machine learning for vaccine authenticity screening. *Npj Vaccines* **9**, 1–14 (2024).
- World Health Organization. WHO lists two additional COVID-19 vaccines for emergency use and COVAX roll-out. <https://www.who.int/news/item/15-02-2021-who-lists-two-additional-covid-19-vaccines-for-emergency-use-and-covax-roll-out> (2021).
- World Health Organization. *Medical Product Alert N°5/2021: Falsified COVISHIELD vaccine (Update)*. <https://www.who.int/news/item/31-08-2021-medical-product-alert-n-5-2021-falsified-covishield-vaccine> (2021).
- Vickers, S. et al. Field detection devices for screening the quality of medicines: a systematic review. *BMJ Glob. Health* **3**, e000725 (2018).
- Newton, P. N., Green, M. D., Fernández, F. M., Day, N. P. J. & White, N. J. Counterfeit anti-infective drugs. *Lancet Infect. Dis.* **6**, 602–613 (2006).
- Singhal, N., Kumar, M., Kanaujia, P. K. & Virdi, J. S. MALDI-TOF mass spectrometry: an emerging technology for microbial identification and diagnosis. *Front. Microbiol.* **6**, 791 (2015).
- Elbehiry, A. et al. How MALDI-TOF mass spectrometry technology contributes to microbial infection control in healthcare settings. *Vaccines* **10**, 1881 (2022).
- Nilsson, E. J. et al. Mechanisms of crystallisation in polysorbates and sorbitan esters. *CrystEngComm* **22**, 3840–3853 (2020).
- Bellina, B., Merthe, D. J. & Kresin, V. V. Proton transfer in histidine-tryptophan heterodimers embedded in helium droplets. *J. Chem. Phys.* **142**, 114306 (2015).

30. Hvattum, E., Yip, W. L., Grace, D. & Dyrstad, K. Characterization of polysorbate 80 with liquid chromatography mass spectrometry and nuclear magnetic resonance spectroscopy: Specific determination of oxidation products of thermally oxidized polysorbate 80. *J. Pharm. Biomed. Anal.* **62**, 7–16 (2012).
31. Yang, Z. China's Paxlovid cyber scams are everywhere. *MIT Technology Review* <https://www.technologyreview.com/2023/01/11/1066605/chinas-paxlovid-cyber-scams/> (2023).
32. Frosch, T. et al. Counterfeit and substandard test of the antimalarial tablet Riamet® by means of raman hyperspectral multicomponent analysis. *Molecules* **24**, 3229 (2019).
33. Korcok, M. Counterfeit drugs latest public health hazard in US. *CMAJ Can. Med. Assoc. J.* **169**, 223 (2003).
34. Hindustan Times. Amikacin may have been used at fake Covid-19 vaccination camp in Kolkata. <https://www.hindustantimes.com/india-news/amikacin-may-have-been-used-at-fake-covid-19-vaccination-camp-in-kolkata-101624564851378.html> (2021).
35. Serum Institute of India. COVISHIELD FAQs. https://www.seruminstitute.com/health_faqs_covishield.php#faq1 (2021).
36. Gibb, S. & Strimmer, K. MALDIquant: a versatile R package for the analysis of mass spectrometry data. *Bioinformatics* **28**, 2270–2271 (2012).
37. Pang, Z. et al. Using MetaboAnalyst 5.0 for LC–HRMS spectra processing, multi-omics integration and covariate adjustment of global metabolomics data. *Nat. Protoc.* **17**, 1735–1761 (2022).
38. Ralbovsky, N. M. & Smith, J. P. Machine learning for prediction, classification, and identification of immobilized enzymes for biocatalysis. *Pharm. Res.* **40**, 1479–1490 (2023).
39. R Core Team. R: A language and environment for statistical computing. R Foundation for Statistical Computing, Vienna, Austria. <https://www.R-project.org/> (2021).
40. Thévenot, E. A., Roux, A., Xu, Y., Ezan, E. & Junot, C. Analysis of the human adult urinary metabolome variations with age, body mass index, and gender by implementing a comprehensive workflow for univariate and OPLS statistical analyses. *J. Proteome Res.* **14**, 3322–3335 (2015).
41. The Wall Street Journal. Pfizer identifies fake COVID-19 shots abroad as criminals exploit vaccine demand. <https://www.livemint.com/companies/news/pfizer-identifies-fake-covid-19-shots-abroad-as-criminals-exploit-vaccine-demand-11619024998051.html> (2021).
- the Indonesian Education Scholarship (Beasiswa Pendidikan Indonesia) from the Ministry of Education, Culture, Research, and Technology of the Republic of Indonesia (Kemendikbudristek) within a funding scheme from Indonesia Endowment Fund for Education (LPDP). B.G and L.G.F were partly supported by the Oxford Glycobiology Endowment. This research was funded in part, by the Wellcome Trust [220211/Z/20/Z, 202935/Z/16/Z, 222506/Z/21/Z]. For the purpose of Open Access, the author has applied a CC BY public copyright license to any Author Accepted Manuscript version arising from this submission. The funder played no role in the study design, data collection, analysis and interpretation of data, or the writing of this manuscript.

Author contributions

N.Z, J.M, P.N.N and B.G designed the study. B.Y.A, R.C, L.G.F, B.G, T.B, and FP performed the experiments and/or data analysis. B.Y.A prepared the original draft. R.C, T.B, L.G.F, J.W-T, M.D, S.M, Q.L, S.B, S.R.C, K.D.P, S.G, K.V.A, S.D, H.A.M, R.S, R.K, A.M, J-P.C, FP, C.C, P.M, J.M, P.N.N, N.Z, FP, and B.G contributed to the writing, reviewing, and editing of the manuscript. S.R.C, K.D.P, S.G, R.K, and A.M provided the vaccines. P.N.N, N.Z, J.M and P.M were involved in funding acquisition. N.Z, J.M, B.G and P.N.N were involved in project management. All authors read and approved the final manuscript.

Competing interests

SRC, KDP & SG are employees of the Serum Institute of India Pvt. Ltd, RS is an employee of Agilent Technologies LDA UK and J-PC is an employee of bioMérieux. No other authors have competing interests.

Additional information

Supplementary information The online version contains supplementary material available at <https://doi.org/10.1038/s41541-024-01051-3>.

Correspondence and requests for materials should be addressed to Paul N. Newton or Bevin Gangadharan.

Reprints and permissions information is available at <http://www.nature.com/reprints>







Publisher's note Springer Nature remains neutral with regard to jurisdictional claims in published maps and institutional affiliations.

Open Access This article is licensed under a Creative Commons Attribution 4.0 International License, which permits use, sharing, adaptation, distribution and reproduction in any medium or format, as long as you give appropriate credit to the original author(s) and the source, provide a link to the Creative Commons licence, and indicate if changes were made. The images or other third party material in this article are included in the article's Creative Commons licence, unless indicated otherwise in a credit line to the material. If material is not included in the article's Creative Commons licence and your intended use is not permitted by statutory regulation or exceeds the permitted use, you will need to obtain permission directly from the copyright holder. To view a copy of this licence, visit <http://creativecommons.org/licenses/by/4.0/>.

© The Author(s) 2025

Acknowledgements

We are grateful to two anonymous donor families and the Oak Foundation who provided dedicated funds to the University of Oxford to support this research. We also thank the Serum Institute of India for the generous provision of the vaccine samples and are grateful to the WHO for facilitating the transfer of the vaccines. We thank the WHO for their grant support to the Rutherford Appleton Laboratory (Ref. 2021/1170671-0). We are very grateful to bioMérieux, for the long-term loan of the Vitek-MS. Furthermore, we would like to thank Sarah Gilbert, Adrian Hill, Andrew Pollard, Michelle Taylor-Siddons, Islip Surgery, Chris Conlon, Ali Amini, Audrey Dubot-Pères, Raymond A. Dwek, the Oxford University Hospitals NHS Foundation Trust, Cathrin Hauk and Kerlijn Van Assche of Oxford University for generous support of this project and expert advice. We also thank Weston Struwe and David Harvey for their expert guidance. S.D acknowledges funding from NIHR Global Research Professorship (NIHR300791). M.D, C.C and P.N.N are supported by the Wellcome Trust (222506/Z/21/Z). B.Y.A is funded by

Benediktus Yohan Arman ^{1,2}, Rebecca Clarke ³, Tehmina Bharucha^{1,2}, Laura Gomez Fernandez^{1,2}, John Walsby-Tickle ³, Michael Deats^{4,5,6}, Sara Mosca ⁷, Qianqi Lin ^{7,15}, Sneha Banerjee⁷, Shrikrishna R. Chunekar⁸, Kundan D. Patil⁸, Sunil Gairola⁸, Susanna Dunachie ^{5,9,10}, Hamid A. Merchant ¹¹, Robert Stokes¹², Rutendo Kuwana¹³, Alexandrine Maes ¹³, Jean-

Philippe Charrier¹⁴, Fay Probert³, Céline Caillet^{4,5,6}, Pavel Matousek^{4,7}, James McCullagh⁸, Paul N. Newton^{4,5,6}, Nicole Zitzmann^{1,2} & Bevin Gangadharan^{1,2}

¹Department of Biochemistry, University of Oxford, OX1 3QU Oxford, UK. ²Kavli Institute for Nanoscience Discovery, University of Oxford, OX1 3QU Oxford, UK. ³Department of Chemistry, University of Oxford, OX1 3TA Oxford, UK. ⁴Medicine Quality Research Group, NDM Centre for Global Health Research, Nuffield Department of Medicine, University of Oxford, Oxford OX3 7LG, UK. ⁵Mahidol-Oxford Tropical Medicine Research Unit, Faculty of Tropical Medicine, Mahidol University, Bangkok 10400, Thailand. ⁶Infectious Diseases Data Observatory, Centre of Tropical Medicine & Global Health, Nuffield Department of Medicine, University of Oxford, Oxford OX3 7LG, UK. ⁷Central Laser Facility, Research Complex at Harwell, STFC Rutherford Appleton Laboratory, UKRI, Harwell Campus, Oxford OX11 0QX, UK. ⁸Serum Institute of India Pvt. Ltd., 212/2, Hadapsar, Pune 411028, India. ⁹Department of Microbiology and Infectious Diseases, Oxford University Hospitals NHS Foundation Trust, Oxford OX3 9DU, UK. ¹⁰NIHR Oxford Biomedical Research Centre, Oxford University Hospitals NHS Foundation Trust, Oxford OX3 9DU, UK. ¹¹Department of Bioscience, School of Health, Sport and Bioscience, University of East London, Water Lane, London E15 4LZ, UK. ¹²Agilent Technologies LDA UK, Becquerel Avenue, Didcot OX11 0RA, UK. ¹³Regulation and Safety Unit, Regulation and Prequalification Department, Access to Medicines and Health Products Division, World Health Organization (WHO), Geneva, Switzerland. ¹⁴Department of Microbiology Research & Development, bioMérieux, Marcy l'Étoile, France. ¹⁵Present address: Hybrid Materials for Opto-Electronics Group, Department of Molecules and Materials, MESA+ Institute for Nanotechnology, Molecules Center and Center for Brain-Inspired Nano Systems, Faculty of Science and Technology, University of Twente, 7500AE Enschede, the Netherlands.

✉ e-mail: paul.newton@ndm.ox.ac.uk; bevin.gangadharan@bioch.ox.ac.uk